Journal of Statistical Planning and Inference 205 (2020) 283–292

Contents lists available at ScienceDirect

Journal of Statistical Planning and Inference

journal homepage: www.elsevier.com/locate/jspi

Combining envelope methodology and aster models for variance reduction in life history analyses

Daniel J. Eck [a,*], Charles J. Geyer [b], R. Dennis Cook [b]

[a] Department of Statistics, University of Illinois, Champaign-Urbana, IL, United States
[b] School of Statistics, University of Minnesota, Minneapolis, MN, United States

ARTICLE INFO

Article history:
Received 29 August 2018
Received in revised form 10 May 2019
Accepted 11 August 2019
Available online 2 September 2019

Keywords:
Darwinian fitness
Fitness landscape
Envelope model
Parametric bootstrap

ABSTRACT

Precise estimation of expected Darwinian fitness, the expected lifetime number of offspring of organism, is a central component of life history analysis. The aster model serves as a defensible statistical model for distributions of Darwinian fitness. The aster model is equipped to incorporate the major life stages an organism travels through which separately may effect Darwinian fitness. Envelope methodology reduces asymptotic variability by establishing a link between unknown parameters of interest and the asymptotic covariance matrices of their estimators. It is known both theoretically and in applications that incorporation of envelope methodology reduces asymptotic variability. We develop an envelope framework, including a new envelope estimator, that is appropriate for aster analyses. The level of precision provided from our methods allows researchers to draw stronger conclusions about the driving forces of Darwinian fitness from their life history analyses than they could with the aster model alone. Our methods are illustrated on a simulated dataset and a life history analysis of *Mimulus guttatus* flowers is provided. Useful variance reduction is obtained in both analyses.

1. Introduction

Life history analysis is the study of a population of organisms as they progress through their lifecycle. A plant or animal's Darwinian fitness – the number of offspring produced over its lifetime – is the primary outcome measure in life history analysis. The estimation of expected Darwinian fitness, the expected lifetime number of offspring an organism has, is one of the most important procedures in evolutionary biology. The importance of life history analyses are not just limited to evolutionary biology, it is important for public policy. With genetic theory and simulation studies, Burger and Lynch (1995) show that, under certain conditions, a changing environment leads to extinction of species. In a field study, Etterson and Shaw (2001) argued that the predicted evolutionary response to predicted rates of climate change are far too slow. In these papers, and all life history analyses of their kind, Darwinian fitness is the response variable. The interesting scientific conclusions are drawn from it.

In many life history analyses, values of expected Darwinian fitness are plotted using a fitness landscape (Lande and Arnold, 1983; Shaw and Geyer, 2010). A fitness landscape is the conditional expectation of Darwinian fitness given phenotypic trait values considered as a function of those values. When fitness is the response variable in a regression model and phenotypic traits are the covariates, the fitness landscape is the regression function. Estimation of this regression function is not a straight forward task since the lifecycles of individual organisms vary in complexity across

* Corresponding author.
E-mail addresses: dje13@illinois.edu (D.J. Eck), charlie@stat.umn.edu (C.J. Geyer), dennis@stat.umn.edu (R.D. Cook).

https://doi.org/10.1016/j.jspi.2019.08.002
0378-3758/

organisms within and between species. Estimation of the fitness landscape began with Lande and Arnold (1983). They use ordinary least squares regression of fitness on phenotypes to estimate the best linear approximation of the fitness landscape and quadratic regression to estimate the best quadratic approximation. Here "best" means minimum variance unbiased, as in the Gauss–Markov theorem. Their use of t and F tests and confidence intervals requires the assumption that fitness is conditionally homoscedastically normally distributed given phenotypic trait values. This assumption is almost always grossly incorrect when one uses a good surrogate for Darwinian fitness (Mitchell-Olds and Shaw, 1987; Shaw et al., 2008).

Aster models (Geyer et al., 2007; Shaw et al., 2008) were designed to fix all of the problems of the Lande and Arnold (1983) approach and of all other approaches to life history analysis (Shaw et al., 2008). The aster model is the state-of-the-art model for life history analyses in which the estimation of expected Darwinian fitness is the primary goal. Aster modeling allows one to combine estimates of selection acting through different components of fitness in a unifying statistical framework to gain insight into overall Darwinian fitness (Siepielski et al., 2011). Geyer et al. (2007), Shaw et al. (2008), Stanton-Geddes et al. (2012), Shaw et al. (2015) and Eck et al. (2015) show various kinds of life history data for which aster models are necessary. Assumptions for aster models are given in Section 2.

In this paper, we demonstrate an efficient approach to computing expected Darwinian fitness by combining a variance reduction technique called "envelope methodology" (Cook et al., 2010; Cook and Zhang, 2015; Su and Cook, 2011) with aster models to estimate the fitness landscape in life history analysis. The primary emphasis is that this combination of methods estimates the fitness landscape with less variability than is possible with aster models alone. We first show how existing envelope estimators constructed from the 1D algorithm (Cook and Zhang, 2015, 2016; Zhang and Mai, 2018) can reduce variability in estimation of the fitness landscape. We then develop a new envelope estimator that avoids the potential numerical pitfalls of the 1D algorithm. Variance reduction is assessed using parametric bootstrap techniques in Efron (2014, Section 4). These bootstrap algorithms account for variability in model selection. Our methodology provides the most precise estimation of expected Darwinian fitness to date. Researchers using our methods can therefore draw stronger conclusions about the driving forces of Darwinian fitness from their life history analyses.

In a life history analysis of *M. guttatus* flowers and a simulated example, we show that our methodology leads to variance reduction in estimation of expected Darwinian fitness when compared with analyses that use aster models alone. We show that this variance reduction leads to sharper scientific inferences about the potential causes of Darwinian fitness in the *M. guttatus* life history analysis. Our examples are fully reproducible, and the calculations necessary for their reproduction are included in an accompanying technical report (Eck et al., 2018).

2. The aster model

Aster models are regular full exponential families. Parameters are estimated by maximum likelihood. If Y is the response vector, $\mu = E(Y)$ is the saturated model mean value parameter, and M is the model matrix for an unconditional canonical affine submodel, then the maximum likelihood estimate of μ satisfies $M^T\hat{\mu} = M^T y$ (Geyer et al., 2007, Section 3.2). $\tau = M^T\mu$ is the submodel mean value parameter (Geyer et al., 2007, Section 2.4). Likelihood ratio tests for model comparison and confidence intervals for all parameters are based on the usual asymptotics and Fisher information are provided by R package `aster` (Geyer, 2017a). In particular, for this article we need to know that $\hat{\tau} = M^T y$ is a minimum variance unbiased estimator of the parameter it estimates and its exact variance matrix is the Fisher information matrix for the submodel canonical parameter β (the vector of regression coefficients). That is, in the usual asymptotics of maximum likelihood for this parameter the mean and variance are exact not approximate; only the normal distribution is approximate.

The aster model is a directed acyclic graphical model (Lauritzen, 1996, Section 3.2.3) in which the joint density is aproduct of conditional densities that are specified by the arrows depicted in the graph. Lines that appear in the graph specify nodes which are dependent. For example, an organism may have multiple paths in their life history and can only go down one of them (Eck et al., 2015). The aster model follows six assumptions which are: A1 The graph of arrows is acyclic. A2 In the graph of lines every connected component is a complete graph, which is called a *dependence group*. A3 Every node in a dependence group with more than one node has the same predecessor (there is an arrow from the predecessor to each node in the group). Every dependence group consisting of exactly one node has at most one predecessor. A4 The joint distribution is the product of conditional distributions, one conditional distribution for each dependence group. A5 Predecessor is sample size, meaning each conditional distribution is the distribution of the sum of N independent and identically distributed random vectors, where N is the value of the predecessor, the sum of zero terms being zero. A6 The conditional distributions are exponential families having the components of the response vector for the dependence group as their canonical statistics. Assumptions A5 and A6 mean for an arrow $y_k \to y_j$ that y_j is the sum of independent and identically distributed random variables from the exponential family for the arrow and there are y_k terms in the sum (the sum of zero terms is zero). These assumptions imply that the joint distribution of the aster model is an exponential family (Geyer et al., 2007, Section 2.3). Three of these assumptions have a clear biological meaning as well. Assumptions A1 through A3 restrict an individual from revisiting life stages that have come to pass. Assumption A5 implies that dead individuals remain dead and have no offspring through the course of the study.

As an example of an analysis using aster models consider a population of *Echinacea angustifolia* plants. These perennial plants typically live between 10 and 20 years. Individual *E. angustifolia* go through several life stages leading

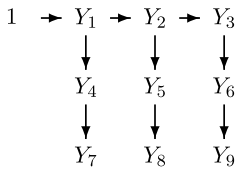

Fig. 1. Graphical structure of the aster model for one individual in the *E. angustifolia* data (Geyer et al., 2007). The top layer corresponds to survival; these random variables are Bernoulli. The middle layer corresponds to flowering; these random variables are also Bernoulli. The bottom layer corresponds to flower head counts; these random variables are zero-truncated Poisson.

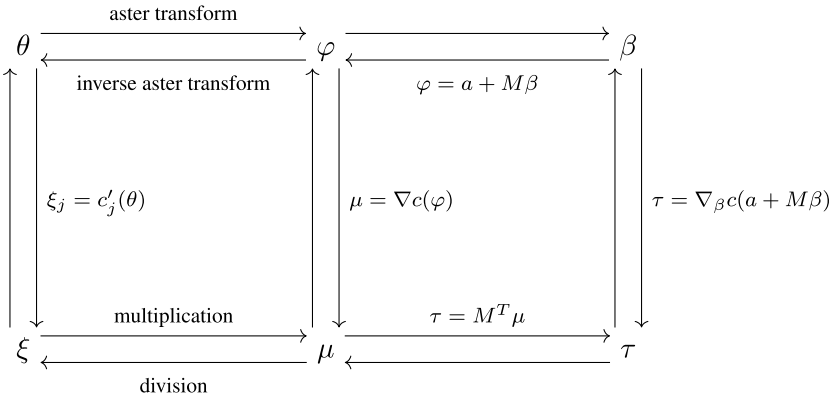

Fig. 2. A depiction of the transformations necessary to change aster model parameterizations. These transformations are all invertible. Arrows going in opposite directions specify transformations and their inverses. M is a known model matrix of full column rank, a is a known offset vector, and c is the cumulant function for the unconditional aster model. Unlabeled arrows represent transformations that need to be evaluated using optimization software in the `aster2` package.

to reproduction at each year they live. A plant that reproduces in any given year had to survive, flower, produce seeds, and have seeds germinate in that year. Darwinian fitness for these plants is the total number of germinating seeds over the course of the plant's life. In the original aster analysis of *E. angustifolia* (Geyer et al., 2007), life history information for survival, flowering, and number of flower heads was collected over three years. No information for seed number or germinating seeds was collected in this study. Total flower head count over the study duration of three years serves as the best possible surrogate to Darwinian fitness in this analysis.

A graph of the lifecycle for one individual which corresponds to the aster model is shown in Fig. 1. The graphical representation of the lifecycle immediately satisfies A1 through A3. There are nine response variables per individual. The first three indicate survival in each of three years. The next three indicate flowering conditional on survival (zero is no flowers, one is some flowers). The last three are flower head counts conditional on successful flowering. The conditional distributions are Bernoulli for the indicator variables (first six) and zero-truncated Poisson for the rest (last three). These are all exponential families with specifications that satisfy assumptions A4 through A6. We can therefore use aster models to study expected total flower head count over the study duration (our best possible surrogate to Darwinian fitness) in this population of *E. angustifolia*.

The aster models that we have discussed up to this point are saturated, having one parameter per component of the response vector, and are not useful. Hence, as with linear and generalized linear models, canonical affine submodels are used with change of parameter $\varphi = a + M\beta$, where φ is the saturated model parameter vector (linear predictor in the terminology of generalized linear models), β is the submodel parameter ("coefficients" in R terminology), a is the offset vector, and M is the model matrix. The aster submodel has log likelihood

$$l(\beta) = \langle M^T Y, \beta \rangle - c(a + M\beta)$$

where Y is the response vector and $c(\cdot)$ is the cumulant function of the exponential family. All of the parameterizations of aster models and their transformations are displayed in the middle and right columns of Fig. 2. For completeness, the parameters in the left column of Fig. 2 correspond to conditional aster models which are not discussed here.

There are three parameters of interest that are present in the aster analyses we consider (see Geyer, 2010 and Eck et al., 2018 for more detail on aster model parameterizations). These parameterizations are (a) the aster submodel canonical parameter vector $\beta \in \mathbb{R}^p$, (b) the aster submodel mean-value parameter vector $\tau \in \mathbb{R}^p$, (c) the saturated aster model mean-value parameter vector $\mu \in \mathbb{R}^m$, where m is the number of individuals sampled multiplied by the number of nodes in the aster graph.

These three parameterizations are all linked via invertible 1–1 transformations when the model matrix M is of full rank. The usual asymptotics of maximum likelihood estimation give

$$\sqrt{n}\left(\hat{\tau} - \tau\right) \xrightarrow{d} N\left(0,\ \Sigma\right), \tag{1}$$

where $\Sigma = \mathrm{Var}(M^T Y)$ is the Fisher information matrix associated with the canonical parameter vector β. The maximum likelihood estimator of β is asymptotically normal with variance given by Σ^{-1}. From (1) and the delta method we can obtain the asymptotic distribution for any differentiable function of $\hat{\tau}$. The asymptotic distribution for a differentiable function g of $\hat{\tau}$ is

$$\sqrt{n}\left\{g(\hat{\tau}) - g(\tau)\right\} \xrightarrow{d} N\left\{0,\ \nabla g(\tau)\Sigma\nabla g(\tau)^T\right\}. \tag{2}$$

In particular, the asymptotic distribution of estimated expected Darwinian fitness is of interest. Let $h(\mu)$ be expected Darwinian fitness. Both β being a function of τ and $\mu = \nabla c(a + M\beta)$ imply that $g(\tau) = h\Big[\nabla c\big\{a + Mf(\tau)\big\}\Big]$ is expected Darwinian fitness as a function of τ and is differentiable if h is differentiable. The estimator $g(\hat{\tau})$ has asymptotic distribution given by (2). We have the potential to do better through the incorporation of envelope methodology.

3. Incorporation of envelope methodology

Aster model estimates of expected Darwinian fitness may be too variable to be useful, and in consequence we may not be able to statistically distinguish estimates of expected Darwinian fitness over the fitness landscape. We address this problem through the incorporation of envelope methodology into the aster modeling framework.

Envelope models were developed originally as a variance reduction tool for the multivariate linear regression model. In this article we focus on envelope methodology for general vector-valued parameter estimation (Cook and Zhang, 2015). Envelope methodology has the potential to reduce the variability of any $\sqrt{n}$-consistent asymptotically normal distributed consistent estimator. We now define the envelope subspace. Let υ be a parameter of interest and suppose that $\hat{\upsilon}$ is a $\sqrt{n}$-consistent estimator of υ with asymptotic covariance matrix $\Sigma_{\upsilon,\upsilon}$. Let $\mathcal{T} = \mathrm{span}(\upsilon) = \{a\upsilon : a \in \mathbb{R}\}$. The envelope subspace $\mathcal{E}_{\Sigma_{\upsilon,\upsilon}}(\mathcal{T})$ is defined as the intersection of all reducing subspaces of $\Sigma_{\upsilon,\upsilon}$ that contain T (a reducing subspace is a sum of eigenspaces if all eigenvalues of Σ have multiplicity one). The envelope space satisfies both

$$\mathcal{T} \subset \mathcal{E}_{\Sigma_{\upsilon,\upsilon}}(\mathcal{T}), \qquad \Sigma_{\upsilon,\upsilon} = P_{\mathcal{E}}\Sigma_{\upsilon,\upsilon}P_{\mathcal{E}} + Q_{\mathcal{E}}\Sigma_{\upsilon,\upsilon}Q_{\mathcal{E}};$$

where $P_{\mathcal{E}}$ is the projection into the envelope subspace and $Q_{\mathcal{E}}$ is the projection into the orthogonal complement. In coordinate form, these two envelope conditions are

$$\mathcal{T} \subset \mathrm{span}(\Gamma), \qquad \Sigma_{\upsilon,\upsilon} = \Gamma\Omega\Gamma^T + \Gamma_o\Omega_o\Gamma_o^T;$$

where (Γ, Γ_o) is a partitioned orthogonal matrix, the columns of Γ are a basis for $\mathcal{E}_{\Sigma_{\upsilon,\upsilon}}(\mathcal{T})$, and the dimensions of the positive definite matrices Ω and Ω_o are such that the matrix multiplications are defined. The quantities $P_{\mathcal{E}}\Sigma_{\upsilon,\upsilon}P_{\mathcal{E}}$ and $\Gamma\Omega\Gamma^T$ are often referred to as 'material information' in the envelope literature (Cook et al., 2010; Cook and Zhang, 2015) since they represent the portion of variability that is necessary for the task of estimating υ. Similarly, $Q_{\mathcal{E}}\Sigma_{\upsilon,\upsilon}Q_{\mathcal{E}}$ and $\Gamma_o\Omega_o\Gamma_o^T$ are referred to as 'immaterial information' since they represent extraneous variability.

Intuitively, the envelope estimator reduces variability in estimation at no cost to consistency. An illuminating depiction and explanation of how an envelope analysis increases efficiency in multivariate linear regression problems was given by Su and Cook (2011, pgs. 134–135). The same intuition applies to envelope methodology of Cook and Zhang (2015). In applications, there is a cost to estimate $u = \dim\left\{\mathcal{E}_{\Sigma_{\upsilon,\upsilon}}(\mathcal{T})\right\}$ and Γ. With the basis matrix Γ estimated, we can then assess the variance reduction of the envelope estimator through the parametric bootstrap.

The 1D algorithm (Cook and Zhang, 2015, Algorithm 2) estimates a basis matrix Γ for $\mathcal{E}_{\Sigma_{\upsilon,\upsilon}}(\mathcal{T})$ at a user-supplied envelope dimension u. The estimate of Γ is obtained by providing $\widehat{\Sigma}_{\upsilon,\upsilon}$ and $\hat{\upsilon}\hat{\upsilon}^T$ as inputs into the 1D algorithm. The resulting estimator of Γ obtained from the 1D algorithm, $\widehat{\Gamma}_u$, gives a $\sqrt{n}$ consistent estimator $P_{\hat{\mathcal{E}}}$ of the projection onto the envelope subspace $P_{\mathcal{E}}$ (Cook and Zhang, 2015). The 1D algorithm can be used to estimate u consistently (Zhang and Mai, 2018, Theorem 2).

Define $\hat{\upsilon}_{1\mathrm{D}} = P_{\hat{\mathcal{E}}}\hat{\upsilon}$ to be the envelope estimator of υ where υ are parameters that link the estimation of expected Darwinian fitness to covariates of interest. We write $\tau = (\gamma^T, \upsilon^T)^T$ where γ are aster model parameters not linking covariates to the estimation of Darwinian fitness. The envelope estimator of τ is given as

$$\hat{\tau}_{1\mathrm{D}} = \begin{pmatrix} \widehat{\gamma} \\ \hat{\upsilon}_{1\mathrm{D}} \end{pmatrix} = \begin{pmatrix} I & 0 \\ 0 & P_{\hat{\mathcal{E}}} \end{pmatrix} M^T Y = M_{1\mathrm{D}}^T Y, \qquad M_{1\mathrm{D}} = M\begin{pmatrix} I & 0 \\ 0 & P_{\hat{\mathcal{E}}} \end{pmatrix}.$$

The model matrix $M_{1\mathrm{D}}$ corresponds to the aster model that incorporates the envelope structure within it instead of the original aster model with model matrix M.

Proposition 1. *The envelope estimator $\hat{\tau}_{1D}$ is a maximum likelihood estimator of τ corresponding to the aster model fit with estimated model matrix M_{1D}.*

Proof. We have $l_{\text{env}}(\beta) = \langle Y, M_{1D}\beta\rangle - c(M_{1D}\beta) = \langle M_{1D}^T Y, \beta\rangle - c(M_{1D}\beta)$. and $\nabla_\beta l(\beta) = M_{1D}^T Y - \nabla_\beta c(M_{1D}\beta)$. Setting $\nabla_\beta l(\beta) = 0$ and solving for β yields $\nabla_\beta c(M_{1D}\beta)|_{\beta=\hat{\beta}} = M_{1D}^T Y = \hat{\tau}_{1D}$. □

This proposition justifies the use of the transformations to switch between maximum likelihood estimators of the different aster model parameterizations. We compare envelope dimensions u by transforming envelope estimators of τ to envelope estimators of β and then evaluate the log likelihood at the envelope estimator of β. The randomness inherent in M_{1D} is non-problematic in most applications. This is because the 1D algorithm provides a $\sqrt{n}$-consistent envelope estimator of υ even when u is estimated. Inferences about aster model parameters implicitly assume that n is large enough for the asymptotic normality to be a good approximation for the distribution of maximum likelihood estimators.

We then compute an envelope estimator of expected Darwinian fitness $g(\tau)$ using the aster model with model matrix M_{1D}. Note that the model matrix M_{1D} is not of full column rank. Therefore the transformations in Fig. 2 used to switch between aster model parameterizations are not 1–1. In particular, many distinct estimates of β map to $\hat{\tau}_{1D}$. Each of these distinct estimated values of β maps to the same estimate of $M_{1D}\beta$, which in turn maps to a common estimate of expected Darwinian fitness. The loss of 1–1 transformations is not an issue in this case.

Our estimator of estimated expected Darwinian fitness is given by Efron (2014, equation (4.5)), with $g(\cdot)$ replacing $t(\cdot)$. Steps for this algorithm are given in Algorithm 1. When the top-level of our bootstrap procedure (Steps 1 through 4 in Algorithm 1) has run for B iterations, we obtain the envelope estimator

$$\hat{g}_{1D} = \frac{1}{B}\sum_{b=1}^{B} g\left\{\hat{\tau}_{1D}^{(b)}\right\}. \tag{3}$$

The envelope estimator $\hat{g}_{1D}$ implicitly behaves as a weighted average with the weights reflecting the likelihood of observing a particular estimated value of u, $\hat{\upsilon}_{1D}$, and M_{1D}. The value of u is estimated with either the Bayesian information criterion or Akaike information criterion at every iteration of the parametric bootstrap. The intuition is that the averaging in $\hat{g}_{1D}$ will smooth out variability due to the estimating u with our chosen model selection criterion. Variability of $\hat{g}_{1D}$ is estimated using the double bootstrap technique in Efron (2014, Section 4), with steps shown below in Algorithm 1. This bootstrap technique accounts for all estimation error, including model selection error. The reason it accounts for all estimation error, is that all estimation, including model selection is done in each iteration of the bootstrap (nothing estimated is ever treated as known in bootstrap iterations).

Algorithm 1. Parametric bootstrap for assessing the variability of the envelope estimator $\hat{g}_{1D}$:

1. Fit the aster model to the data and obtain $\hat{\upsilon}$ and $\widehat{\Sigma}_{\upsilon,\upsilon}$ from the aster model fit.
2. Choose a model selection criterion. Compute the envelope estimator of υ in the original sample, given as $\hat{\upsilon}_{1D} = P_{\hat{\mathcal{E}}}\hat{\upsilon}$ where $P_{\hat{\mathcal{E}}}$ is obtained from the 1D algorithm and the chosen model selection criterion.
3. Perform a parametric bootstrap by generating samples from the distribution of the aster submodel evaluated at $\hat{\tau}_{1D} = (\hat{\gamma}^T, \hat{\upsilon}_{1D}^T)^T$. For $b = 1, \ldots, B$ of the procedure:
   - (ci) Compute $\hat{\tau}^{(b)}$ and $\widehat{\Sigma}_{\upsilon,\upsilon}^{(b)}$ from the aster model fit to the resampled data.
   - (cii) Compute $P_{\hat{\mathcal{E}}}^{(b)}$ as done in Step (b).
   - (ciii) Compute $\hat{\tau}_{1D}^{(b)} = \left\{\hat{\gamma}^{(b)^T}, \hat{\upsilon}_{1D}^{(b)^T}\right\}^T$ and $g\left\{\hat{\tau}_{1D}^{(b)}\right\}$.
4. The bootstrap estimator of expected Darwinian fitness is the average of the envelope estimators computed in Step 3c. This completes the first part of the bootstrap procedure.
5. At $k = 1, \ldots, K$, for each $b = 1, \ldots, B$ we:
   - (ei) Generate data from the distribution of the aster submodel evaluated at $\hat{\tau}_{1D}^{(b)}$.
   - (eii) Perform Steps (ci) through (ciii) with respect to the dataset obtained in Step (ei) to calculate both $\hat{\tau}_{1D}^{(b)^{(k)}}$ and $g\left\{\hat{\tau}_{1D}^{(b)^{(k)}}\right\}$.
6. Compute both $\hat{g}_{1D}$ and the standard deviation in Efron (2014, equation (4.15)).

4. A direct envelope estimator using reducing subspaces

We propose a new way of constructing envelope estimators provided that the eigenvalues of $\Sigma_{\upsilon,\upsilon}$ have multiplicity one. In this section, envelope estimators are constructed directly from the reducing subspaces of $\widehat{\Sigma}_{\upsilon,\upsilon}$. Uniqueness of the eigenvalues of $\Sigma_{\upsilon,\upsilon}$ implies that its reducing subspaces are sums of its eigenspaces. Let $\mathcal{G}$ be a reducing subspace of $\Sigma_{\upsilon,\upsilon}$. Define $\Gamma_{\mathcal{G}}$ and $P_{\mathcal{G}}$ as the basis matrix for $\mathcal{G}$ and the projection onto $\mathcal{G}$ respectively. Let $\widehat{\mathcal{G}}$ be the estimator of the reducing subspace $\mathcal{G}$, where $\widehat{\mathcal{G}}$ is the direct sum of a subset of the 1 dimensional eigenspaces of $\widehat{\Sigma}_{\upsilon,\upsilon}$. In applications, eigenvalues of $\widehat{\Sigma}_{\upsilon,\upsilon}$ are almost always unique. Define $\widehat{\Gamma}_{\widehat{\mathcal{G}}}$ and $\widehat{P}_{\widehat{\mathcal{G}}} = \widehat{\Gamma}_{\widehat{\mathcal{G}}}\widehat{\Gamma}_{\widehat{\mathcal{G}}}^T$ as estimators of $\Gamma_{\mathcal{G}}$, and $P_{\mathcal{G}}$ respectively. The basis matrix $\widehat{\Gamma}_{\widehat{\mathcal{G}}}$ is constructed from the eigenvectors of $\widehat{\Sigma}_{\upsilon,\upsilon}$. We now define the envelope estimator of υ constructed from reducing subspaces.

Definition 1. The envelope estimator of υ constructed from the reducing subspaces $\mathcal{G}$ is defined to be $\hat{\upsilon}_{\text{env}} = \widehat{P}_{\widehat{\mathcal{G}}}\hat{\upsilon}$.

The reducing subspaces of $\widehat{\Sigma}_{\upsilon,\upsilon}$ are $\sqrt{n}$ consistent estimators of the reducing subspaces of $\Sigma_{\upsilon,\upsilon}$. Therefore $\widehat{\Gamma}_{\widehat{\mathcal{G}}}$, $\widehat{P}_{\widehat{\mathcal{G}}}$, and the corresponding estimator $\widehat{P}_{\widehat{\mathcal{G}}}\hat{\upsilon}$ are $\sqrt{n}$ consistent estimators of $\Gamma_{\mathcal{G}}$, $P_{\mathcal{G}}$, and υ respectively. The envelope estimator of τ constructed by reducing subspaces is given by

$$\hat{\tau}_{\text{env}} = \begin{pmatrix} \widehat{\gamma} \\ \hat{\upsilon}_{\text{env}} \end{pmatrix} = \begin{pmatrix} I & 0 \\ 0 & \widehat{P}_{\widehat{\mathcal{G}}} \end{pmatrix} M^T Y = M_{\text{env}}^T Y, \qquad M_{\text{env}} = M \begin{pmatrix} I & 0 \\ 0 & \widehat{P}_{\widehat{\mathcal{G}}} \end{pmatrix}.$$

The model matrix M_{env} corresponds to the aster model that incorporates the envelope structure obtained from the reducing subspaces of $\widehat{\Sigma}_{\upsilon,\upsilon}$. We have a similar result as Proposition 1 for the aster model with model matrix M_{env}.

Proposition 2. *The envelope estimator $\hat{\tau}_{env}$ is a maximum likelihood estimator of τ corresponding to the aster model fit with estimated model matrix M_{env}.*

The proof of Proposition 2 follows the same steps as the proof for Proposition 1. There is a close connection between envelope estimation using reducing subspaces and envelope estimation using the 1D algorithm. In the population, $\hat{\upsilon}_{\text{env}} = \hat{\upsilon}_{\text{1D}}$. The connection between both estimation methods exists in finite samples as seen in Theorem 1. In preparation, define orthogonal matrices $\widehat{O}_u = \left(\widehat{\Gamma}_u, \widehat{\Gamma}_{uo}\right)$, $\widehat{O}_{\widehat{\mathcal{G}}} = \left(\widehat{\Gamma}_{\widehat{\mathcal{G}}}, \widehat{\Gamma}_{\widehat{\mathcal{G}}o}\right)$, and $\widehat{O} = \widehat{O}_{\widehat{\mathcal{G}}}\widehat{O}_u^T$. The matrices $\widehat{\Gamma}_{\widehat{\mathcal{G}}}$, $\widehat{\Gamma}_{\mathcal{G}o}$, $\widehat{\Gamma}_u$, and $\widehat{\Gamma}_{uo}$ converges in probability to $\Gamma_{\mathcal{G}}$, $\Gamma_{\mathcal{G}o}$, Γ_u, and Γ_{uo} respectively. Now $\Gamma_{\mathcal{G}}^T\Gamma_u$ and $\Gamma_{\mathcal{G}o}^T\Gamma_{uo}$ are both 0–1 valued rotation matrices and $\Gamma_{\mathcal{G}}^T\Gamma_{uo} = \Gamma_{\mathcal{G}o}^T\Gamma_u = 0$. These facts imply that $\widehat{O}$ converges in probability to a 0–1 valued rotation matrix. We will assume that $\widehat{O} \xrightarrow{p} I$ without loss of generality.

Theorem 1. *The basis matrix $\widehat{\Gamma}_{\widehat{\mathcal{G}}}$ is the output of the 1D algorithm with inputs $\widehat{M} = \widehat{O}\widehat{\Sigma}_{\upsilon,\upsilon}\widehat{O}^T$ and $\widehat{U} = \widehat{O}\hat{\upsilon}\hat{\upsilon}^T\widehat{O}^T$ at dimension u.*

Proof. Let $\widehat{M}_2 = \widehat{\Sigma}_{\upsilon,\upsilon}$ and $\widehat{U}_2 = \hat{\upsilon}\hat{\upsilon}^T$. Similar to the proof of Cook and Zhang (2016, Proposition 6), let

$$\begin{aligned} Q_n(g) &= -n/2\log(g^T\widehat{O}\widehat{M}_2\widehat{O}^T g) - n/2\log\left[g^T\left\{\widehat{O}\left(\widehat{M}_2 + \widehat{U}_2\right)\widehat{O}^T\right\}^{-1} g\right] \\ &\quad + n\log(g^T g) \\ &= -n/2\log(g^T\widehat{O}\widehat{M}_2\widehat{O}^T g) - n/2\log\left\{g^T\widehat{O}\left(\widehat{M}_2 + \widehat{U}_2\right)^{-1}\widehat{O}^T g\right\} \\ &\quad + n\log(g^T\widehat{O}\widehat{O}^T g). \end{aligned}$$

Now let $\hat{v}_k$, $k = 1, \ldots, u$ be the kth column of $\widehat{\Gamma}_{\mathcal{G}}$ and define $A \in \mathbb{R}^{p\times p}$ to be a matrix of 0's with 1's occupying the first k diagonal entries. Then

$$\begin{aligned} Q_n(\hat{v}_k) &= -n/2\log(\hat{v}_k^T\widehat{O}\widehat{M}_2\widehat{O}^T\hat{v}_k) - n/2\log\left\{\hat{v}_k^T\widehat{O}\left(\widehat{M}_2 + \widehat{U}_2\right)^{-1}\widehat{O}^T\hat{v}_k\right\} \\ &\quad + n\log(\hat{v}_k^T\widehat{O}^T\widehat{O}\hat{v}_k) \\ &= -n/2\log(A_k\widehat{O}_u\widehat{M}_2\widehat{O}_u^T A_k) - n/2\log\left\{A_k\widehat{O}_u\left(\widehat{M}_2 + \widehat{U}_2\right)^{-1}\widehat{O}_u^T A_k\right\} \\ &\quad + n\log(A_k\widehat{O}_u^T\widehat{O}_u A_k) \\ &= -n/2\log(\hat{g}_{uk}^T\widehat{M}_2\hat{g}_{uk}) - n/2\log\left\{\hat{g}_{uk}^T\left(\widehat{M}_2 + \widehat{U}_2\right)^{-1}\hat{g}_{uk}\right\} \\ &\quad + n\log(\hat{g}_{uk}^T\hat{g}_{uk}) \end{aligned}$$

where $\hat{g}_{uk}$ is the kth column of $\widehat{\Gamma}_u$, the output of the 1D algorithm with $\widehat{M}_2$ and $\widehat{U}_2$ as inputs. Therefore $\hat{v}_k$ is a maximizer of $Q_n(g)$ and this completes the proof. □

Theorem 1 in combination with Zhang and Mai (2018, Theorem 2) allows for us to estimate $\mathcal{G}$ consistently. Thus the variability associated with the estimation of $\hat{\upsilon}_{\text{env}}$ and $\mathcal{G}$ decreases as $n \to \infty$. However in practical applications correct model selection cannot be guaranteed. Therefore the envelope estimator of expected Darwinian fitness $g(\hat{\tau}_{\text{env}})$ has an extra source of variability due to model selection uncertainty. We develop a double bootstrap procedure with steps similar to those in Algorithm 1 to account for variability in model selection. The first level of the bootstrap procedure provides the estimator of expected Darwinian fitness,

$$\hat{g}_{\text{env}} = \frac{1}{B}\sum_{b=1}^{B} g\left\{\hat{\tau}_{\text{env}}^{(b)}\right\}. \tag{4}$$

The same model selection criteria is used to select the reducing subspace used to construct $\hat{\tau}_{\text{env}}^{(b)}$ at every iteration $b = 1, \ldots, B$. The second of level of this bootstrap procedure estimates the variability of (4). The steps for this algorithm

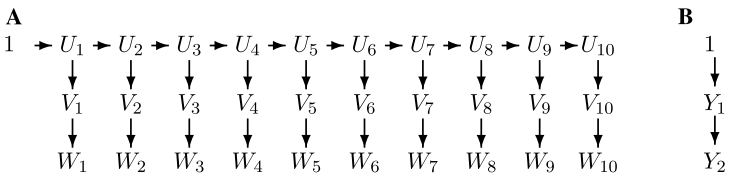

Fig. 3. **(A)** Graphical structure of the aster model for the simulated data in Example 1. The top layer corresponds to survival; these random variables are Bernoulli. The middle layer corresponds to whether or not an individual reproduced; these random variables are also Bernoulli. The bottom layer corresponds to offspring count; these random variables are zero-truncated Poisson. **(B)** Graphical structure of the aster model for the data in Example 2. The first arrow corresponds to survival which is a Bernoulli random variable. The second arrow corresponds to reproduction count conditional on survival which is a zero-truncated Poisson random variable.

are provided in Eck et al. (2018). The utility of our double bootstrap procedure is shown in Section 5.1 where, in that example, there is considerable disagreement between model selection criteria.

When k is small, $\hat{\upsilon}_{\text{env}}$ is preferable to $\hat{\upsilon}_{\text{1D}}$. At any iteration of the 1D algorithm, minimizers of the objective function stated in Cook and Zhang (2015, Algorithm 2) are pulled towards reducing subspaces of $\widehat{\Sigma}_{\upsilon,\upsilon}$. This objective function is non-convex and contains potentially many local minima. The optimizations conducted within the 1D algorithm are sensitive to starting values and can get stuck at these local minima. This undermines the 1D algorithm since it is required that users find global minima for its justification. Unlike the 1D algorithm, the reducing subspace approach does not involve any optimization routines. However when k is moderately large, the computation of all of candidate envelope estimators at each reducing subspace is too computationally intensive, there are $2^k - 1$ possible reducing subspaces in non trivial problems. The 1D algorithm may still be fast when k is moderately large, only $k-1$ optimizations in non trivial problems. In most aster applications k is small since data is obtained through expensive collection methods and fitness landscapes are low-dimensional (Shaw and Geyer, 2010; Eck et al., 2015).

5. Examples

5.1. Simulated data

A population of 3000 organisms was simulated to form the dataset used in this aster analysis. These data were generated according to the graphical structure appearing in panel A of Fig. 3. There are two covariates (z_1, z_2) associated with Darwinian fitness and the aster model selected by the likelihood ratio test is a full quadratic model with respect to these covariates.

We partition τ into $(\gamma^T, \upsilon^T)^T$ where $\gamma \in \mathbb{R}^4$ are nuisance parameters and $\upsilon \in \mathbb{R}^5$ are relevant to the estimation of expected Darwinian fitness. Here, $\upsilon \in \mathbb{R}^5$ because our model is full quadratic in z_1 and z_2. In this example, the true reducing subspace is the space spanned by the first and fourth eigenvectors of the covariance matrix of the parameters of interest estimated from the original data. We begin by considering envelope estimators constructed using the 1D algorithm. The Akaike information criterion and the Bayesian information criterion both select $u = 5$. Envelope methods are not interesting in this case.

We now consider envelope estimators constructed from reducing subspaces. In the original sample, the Bayesian information criterion selects the reducing subspace that is the sum of the first, fourth, and fifth eigenspaces of $\widehat{\Sigma}_{\upsilon,\upsilon}$ numbered in order of decreasing eigenvalues. This suggests that the dimension of the envelope space is $u = 3$. The 1D algorithm and the reducing subspace approach are in disagreement, consistency of model selection is not helpful in this application. We turn to the double parametric bootstrap to estimate $\hat{g}_{\text{env}}$ and the asymptotic variability of $\hat{g}_{\text{env}}$. The Bayesian information criterion is used to select $\mathcal{G}$ at every iteration of the first level of the bootstrap.

The results are seen in Table 1. Table 1 shows seven individuals that had high values of estimated expected Darwinian fitness. Each individual has a unique set of traits. The first two columns display the envelope estimator of expected Darwinian fitness $\hat{g}_{\text{env}}$ and its bootstrapped standard error. The maximum likelihood estimator of expected Darwinian fitness and its bootstrapped standard error are displayed in the third and fourth columns respectively. The ratios of bootstrapped standard errors for $\hat{g}_{\text{MLE}}$ to $\hat{g}_{\text{env}}$ are displayed in the final column. We can see that all of the ratios are greater than 1 which indicates that the envelope estimator of expected Darwinian fitness is less variable than the maximum likelihood estimator.

Contour plots of the ratios of estimated standard errors are displayed in the technical report (Eck et al., 2018). These contour plots show that the envelope estimator of expected Darwinian fitness is less variable than the maximum likelihood estimator for the majority of the observed data. The region where the envelope estimator is less variable includes the values of z_1 and z_2 that maximize estimated expected Darwinian fitness. Variance reduction is also obtained when we use the reducing subspace suggested by the Akaike information criterion. This is also shown in Eck et al. (2018).

Table 1
Comparison of the maximum likelihood estimator and the envelope estimator for seven individuals with high estimates of expected Darwinian fitness in Example 1. The fifth column is the ratio of bootstrapped standard errors for $\hat{g}_{\text{MLE}}$ to $\hat{g}_{\text{env}}$..

$\hat{g}_{\text{env}}$	$\text{se}(\hat{g}_{\text{env}})$	$\hat{g}_{\text{MLE}}$	$\text{se}(\hat{g}_{\text{MLE}})$	Ratio
8.556	0.174	8.701	0.260	1.491
9.014	0.111	8.939	0.135	1.222
7.817	0.414	8.054	0.442	1.069
9.174	0.163	9.193	0.170	1.045
9.018	0.113	9.120	0.128	1.133
8.612	0.162	8.518	0.278	1.709
7.761	0.215	8.096	0.331	1.534

Table 2
Comparison of the maximum likelihood estimator and the envelope estimator for seven individuals with high estimates of expected Darwinian fitness in Example 2. The fifth column is the ratio of bootstrapped standard errors for $\hat{g}_{\text{MLE}}$ to $\hat{g}_{\text{env}}$..

$\hat{g}_{\text{env}}$	$\text{se}(\hat{g}_{\text{env}})$	$\hat{g}_{\text{MLE}}$	$\text{se}(\hat{g}_{\text{MLE}})$	Ratio
9.646	0.326	9.171	0.642	1.973
8.640	0.300	8.887	0.369	1.230
7.659	0.315	7.603	0.361	1.144
7.517	0.539	7.010	0.649	1.205
10.943	0.607	10.475	0.896	1.476
7.329	0.707	6.618	1.038	1.469
7.498	0.521	7.522	0.658	1.263

5.2. *M. guttatus* aster analysis

The yellow monkeyflower *M. guttatus* has been and is currently a well studied flower (Lowry and Willis, 2010; Hall et al., 2006; Ritland and Ritland, 1989; Allen and Sheppard, 1971; Vickery, 1959). *M. guttatus* is a species which comprises many morphologically variable populations growing in moist places such as stream banks, meadows and springs over a range that extends from the Aleutian Islands to Mexico and from the California coast to the Rocky Mountains (Vickery, 1959). The lifecycle of the individual *M. guttatus* flowers, for our life history analysis, is depicted in panel B of Fig. 3. Lowry and Willis (2010) performed a life history analysis of *M. guttatus* using aster models. One of their interests was to determine which levels of genetic background, field site, inversion orientation, and ecotype of the flower are associated with high Darwinian fitness. We show that the set of candidate trait values thought to maximize expected Darwinian fitness is smaller when envelope methodology is incorporated.

Lowry and Willis (2010) collected measurements on 2313 *M. guttatus*. We fit a linear fitness landscape to this data. The parameters $\upsilon \in \mathbb{R}^6$ are relevant to the estimation of expected Darwinian fitness. In the original sample, the Bayesian information criterion leads to a selection of a reducing subspace that is the sum of all eigenspaces of $\widehat{\Sigma}_{\upsilon,\upsilon}$ with the exception of the fourth and fifth eigenspaces. The parametric double bootstrap procedure outlined in Sections 3 and 4 is used to estimate the variability of $\hat{g}_{\text{env}}$ where the Bayesian information criterion is used to select $\mathcal{G}$ at every iteration of the first level of the bootstrap.

Table 2 shows the results for seven individuals that have high values of estimated expected Darwinian fitness through maximum likelihood and envelope estimation. Each individual has a unique set of traits. We see that both methods agree on the trait values that are expected to maximize expected Darwinian fitness. We also see that all of the ratios are greater than 1. More importantly, this variance reduction implies more precise inference in this life history analysis. For example, the envelope estimator can statistically distinguish ($\alpha = 0.05$, unadjusted for multiple comparisons) the second row of Table 2 from the fifth row of Table 2. The combination of envelope methodology into the aster model framework allowed for us to consider a smaller set of traits associated with high Darwinian fitness.

6. Software

This paper is accompanied by an R package `envlpaster` (Eck, 2016), which requires the two R packages for aster models: `aster` (Geyer, 2017a) and `aster2` (Geyer, 2017b), and also a technical report (Eck et al., 2018) that reproduces the examples in this paper and shows how functions in the `envlpaster` package are used.

7. Discussion

One could think to perform envelope methodology with respect to the regression coefficients β instead of τ. However β is not well-defined, one can shift β with an arbitrarily chosen offset vector without changing the value of the mean-value parameters τ and μ. In addition, whenever we have categorical predictors, R software automatically drops one

category when it has an intercept in the formula, but which category it drops is arbitrary and changing which is dropped changes β. Envelope methodology is not invariant to this form of arbitrary shifting. To the best of our knowledge, the exponential family regression applications in the envelope model literature exclusively seek inference about β because this well-definedness issue is not a problem in those applications (Cook et al., 2010; Su and Cook, 2011, 2012; Cook and Su, 2013; Cook et al., 2013; Cook and Zhang, 2015; Cook and Su, 2016; Park et al., 2017; Eck and Cook, 2017). The applications of envelope methods to aster models is therefore outside of the scope of previous applications to exponential family models. Additionally, the methods in this paper can be extended to functions of parameters in generalized linear regression models. Aster model are a generalization of generalized linear regression models (Shaw et al., 2008).

The consequences of potential model selection errors served as the motivation for the implementation of the bootstrap procedure in Eck and Cook (2017). In that article, inferences are only given for a canonical parameter vector in a multivariate linear regression model. We applied the Efron (2014) bootstrap procedures to alleviate possible model selection concerns. However, this particular choice of a bootstrap procedure is not without flaws. Hjort (2014) mentions that Efron does not derive the asymptotic distribution of the final estimator. The literature has not reached a consensus on the appropriate bootstrap procedure to be implemented when bootstrapping depends on data-driven model selection. As the literature currently stands, Efron (2014) provides a reasonable solution to the problem of potential model selection errors in the application of envelope methodology to aster models. The parametric bootstrap does not rely on asymptotic normality since it simulates the exact sampling distribution of the estimator for some parameter value, and the double bootstrap simulates the exact sampling distribution of the estimator for a long list of parameter values (Geyer, 2013).

Our new envelope estimator does not involve any non-convex optimization routines that are both sensitive to starting values and have potential problems with local minima. These computational problems can be detrimental to the performance of the 1D algorithm. The underlying theory of the 1D algorithm justifies the consistency properties of our new envelope estimator. The envelope estimator constructed directly from reducing subspaces is preferred since it possesses the same strengths as the 1D algorithm without its potential numerical pitfalls. However, our estimator can be prohibitively expensive to compute in moderate p problems. In aster analyses p is typically small.

In many life history analyses, specific trait values which are estimated to produce the highest expected Darwinian fitness are of interest. It is common practice to only report such trait values (Shaw and Geyer, 2010; Eck et al., 2015). Such reporting ignores the variability associated with the estimation of expected Darwinian fitness. There are likely many trait values having estimated expected Darwinian fitness that is statistically indistinguishable from the reported values. Our methodology addresses this concern directly. The potential set of candidate traits associated with high values of expected Darwinian fitness is smaller when the combination of envelope methodology into the aster modeling framework is utilized as seen in Eck et al. (2018). Researchers using our methods will have the potential to make stronger inferences about expected Darwinian fitness through our variance reduction techniques.

Acknowledgments

Daniel J. Eck's research is supported by NIH/NIHCD grant 1DP2HD091799-01 (United States). We would like to thank David B. Lowry for providing the dataset used in Example 2, Xin Zhang for the code that implements the 1D algorithm, and Forrest W. Crawford for helpful discussion that led to the strengthening of this paper. We would also like to especially thank Amber Eule-Nashoba for helpful comments on the technical report. We are grateful to two anonymous reviewers whose comments led to improvements in clarity.

References

Allen, W.R., Sheppard, P.M., 1971. Copper tolerance in some californian populations of the monkey flower, *mimulus guttatus*. Proc. R. Soc. London. Ser. B Bio. Sci. 177 (1047), 177–196.

Burger, R., Lynch, M., 1995. Evolution and extinction in a changing environment: A quantitative-genetic analysis. Evolution 49, 151–163.

Cook, R.D., Helland, Z., Su, I.S., 2013. Envelopes and partial least squares regression. J. R. Statist. Soc. B 75, 851–877.

Cook, R.D., Li, B., Chiaromonte, F., 2010. Envelope models for parsimonious and efficient multivariate linear regression. Statist. Sinica 20, 927–1010.

Cook, R.D., Su, Z., 2013. Scaled envelopes: scale-invariant and efficient estimation in multivariate linear regression. Biometrika 100, 939–954.

Cook, R.D., Su, Z., 2016. Scaled predictor envelopes and partial least squares regression. Technometrics 58, 155–165.

Cook, R.D., Zhang, X., 2015. Foundations for envelope models and methods. J. Amer. Statist. Assoc. 110, 599–611.

Cook, R.D., Zhang, X., 2016. Algorithms for envelope estimation. J. Comput. Graph. Statist. 25 (1), 284–300.

Eck, D.J., 2016. R package `envlpaster`, version 0.1–2. http://cran.r-project.org/package=envlpaster.

Eck, D.J., Cook, R.D., 2017. Weighted envelope estimation to handle variability in model selection. Biometrika 104, 743–749.

Eck, D.J., Geyer, C.J., Cook, R.D., 2018. Supporting Data Analysis for "Combining Envelope Methodology and Aster Models for Variance Reduction in Life History Analyses". Technical Report No. 699, School of Statistics, University of Minnesota, http://hdl.handle.net/11299/178384.

Eck, D.J., Shaw, R., Geyer, C.J., Kingsolver, J.G., 2015. An integrated analysis of phenotypic selection on insect body size and development time. Evolution 69, 2525–2532.

Efron, B., 2014. Estimation and accuracy after model selection. J. Amer. Statist. Assoc. 109, 991–1007.

Etterson, J.R., Shaw, R.G., 2001. Constraint to adaptive evolution in response to global warming. Science 294, 151–154.

Geyer, C.J., 2010. A Philosophical Look at Aster Models. Technical Report No. 676, School of Statistics, University of Minnesota, http://purl.umn.edu/57163.

Geyer, C.J., 2013. Asymptotics of maximum likelihood without the LLN or CLT or sample size going to infinity. In: Eaton, L., Jones, G.L., Shen, X. (Eds.), Advances in Modern Statistical Theory and Applications: A Festschrift in honor of Morris. In: IMS Collections, vol. 10, Institute of Mathematical Statistics, Hayward, CA, pp. 1–24.

Geyer, C.J., 2017a. R package `aster` (Aster Models), version 0.9.1. http://cran.r-project.org/package=aster.
Geyer, C.J., 2017b. R package `aster2` (Aster Models), version 0.3. http://cran.r-project.org/package=aster2.
Geyer, C.J., Wagenius, S., Shaw, R.G., 2007. Aster models for life history analysis. Biometrika 94, 415–426.
Hall, M.C., Willis, J.H., Galloway, L., 2006. Divergent selection on flowering time contributes to local adaptation in *Mimulus guttatus* populations. Evolution 60, 2466–2477.
Hjort, N.L., 2014. Discussion of Efron's "Estimation and accuracy after model selection". J. Amer. Statist. Assoc. 109, 1017–1020.
Lande, R., Arnold, S., 1983. The measurement of selection on correlated characters. Evolution 37, 1210–1226.
Lauritzen, S.L., 1996. Graphical Models. Oxford University Press, New York.
Lowry, D.B., Willis, J.H., 2010. A widespread chromosomal inversion polymorphism contributes to a major life-history transition, local adaptation, and reproductive. PLoS Biol. 8 (9), e1000500.
Mitchell-Olds, T., Shaw, R.G., 1987. Regression analysis of natural selection: statistical inference and biological interpretation. Evolution 41, 1149–1161.
Park, Y., Su, Z., Zhu, H., 2017. Groupwise envelope models for imaging genetic analysis. Biometrics.
Ritland, C., Ritland, K., 1989. Variation of sex allocation among eight taxa of the *Mimulus guttatus* species complex (*Scrophulariaceae*). Am. J. Bot. 76 (12), 1731–1739.
Shaw, R.G., Geyer, C.J., 2010. Inferring fitness landscapes. Evolution 64, 2510–2520.
Shaw, R.G., Geyer, C.J., Wagenius, S., Hangelbroek, H., Etterson, J.R., 2008. Unifying life-history analyses for inference of fitness and population growth. Amer. Nat. 172, E35–E47.
Shaw, R.G., Wagenius, S., Geyer, C.J., 2015. The susceptibility of *Echinacea angustifolia* to a specialist aphid: eco-evolutionary perspective on genotypic variation and demographic consequences. J. Ecol. 103, 809–818.
Siepielski, A.M., DiBattista, J.D., Evans, J.A., Carlson, S.M., 2011. Differences in the temporal dynamics of phenotypic selection among fitness components in the wild. Proc. Roy. Soc, B 278 (1711), 1572–1580.
Stanton-Geddes, J., Shaw, R.G., Tiffin, P., 2012. Interactions between soil habitat and geographic range affect plant fitness. PLoS One 7, e36015.
Su, Z., Cook, R.D., 2011. Partial envelopes for efficient estimation in multivariate linear regression. Biometrika 98, 133–146.
Su, Z., Cook, R.D., 2012. Inner envelopes: efficient estimation in multivariate linear regression. Biometrika 99, 687–702.
Vickery, R.K., 1959. Barriers to gene exchange within *Mimulus guttatus*. Evolution 13, 300–310.
Zhang, X., Mai, Z., 2018. Model-free envelope dimension selection. E. J. Statist. 12, 2193–2216.